Experimental operation of drone micro-SAR with efficient time-varying velocity compensation

W.K. Lee✉ and K.W. Lee

Drone platform for synthetic aperture radar (SAR) operation has been little publicised due to the technical constraint of the payload implementation. Multi-rotor drone based SAR is distinguished from the conventional airborne system by the increased sensitivity to turbulences and poor motion stability. Extremely limited power and mass budgets may prevent the use of extra hardware for motion compensation and the difficulty of SAR focusing is aggravated. Feasibility of micro-SAR drone operation is investigated through field tests, where experimental SAR images are acquired over ground targets. Attempts have been made to implement near-real-time compensation for non-uniform motion disturbance. Finally, experimental drone SAR operation is validated through calibrated SAR images.

Introduction: SAR imaging by a multi-rotor platform is a challenging task due to the severe constraints of mass and power budgets and drone SAR development is still in preliminary phase. The difficulty has been demonstrated by the limited performances of unstable range profiles or de-focused SAR processing [1]. Nevertheless, the low-cost portable drones with SAR imaging capability will provide valuable opportunities for agile monitoring in commercial, environmental and military purposes.

Conventional airborne SAR suffers from non-linear motion errors. The problem is further aggravated for lightweight drones as they are highly sensitive to weather conditions and susceptible to the non-linear perturbation of the unstable flying trajectory. The difficulty becomes severe as it should be overcome with limited implementation budget. Previous works on SAR autofocus usually assumes that the velocity deviation is within the fraction of the nominal constant and can be recovered by minimum error estimations [2]. However, small drone platforms are likely to suffer from velocity variations over wide deviation spans and the error correction should be exploited with limited hardware. On-board real-time processing is preferred to relax data storage capacity.

In this Letter, we present a preliminary test result from the experimental SAR operation using a small multi-rotor platform. Due to the system budget constraint, no motion sensor is adopted and SAR autofocusing is performed based on the received raw data only. To relax the computational burden and accommodate near-real-time processing, non-uniform fast Fourier transform (NUFFT) technique is employed to carry out direct interpolations upon the complex drone movements. After non-uniform platform disturbance is compensated by the azimuth phase alignment, the feasibility of the drone SAR operation is verified.

Drone SAR experiment and analysis: A frequency-modulated continuous-wave (FMCW) scheme is advantageous to implement a compact and lightweight SAR system. We have employed a 9.8 GHz X-band software defined transceiver that generates 400 MHz bandwidth chirp signals. The total effective radiated power is 30 dBm at the end of high-gain transmit horn antenna. The received beat signal is digitised with 1 MHz sampling rate. A portable computer is connected to send control signals and store the received SAR raw data. The complete SAR system is mounted on-board a commercial multi-rotor platform that can carry a compact payload up to 5 kg. Fig. 1 shows the FMCW SAR system stowed inside the multi-rotor body. Two horn antennas are mounted under the platform with zero squint angle. The drone platform flies at 50 m altitude and the wind velocity is measured as 3–4 m/s.

In this configuration, the swath width is ~25 m and the resolutions are 0.5 and 0.1 m in range and azimuth, respectively. As the navigation data is not available, the Doppler rate and platform velocity parameters are estimated based on the received raw data only. To reconstruct the parabolic form of the SAR geometry model, prominent scatterers are detected in range compressed data by peak detection. Then its range trajectory is estimated by using random sample consensus (RANSAC) polynomial fitting. Based on the estimated range equation, the geometric parameters are derived that include the slant range of the closest approach, azimuth time and initial velocity. Afterward, a maximum contrast method is conducted for precise velocity estimation.

Four corner reflectors (CRs) are placed as ground targets. Fig. 2*a* shows the range compressed data from CR target 1 in amplitude and phase. The disturbed phase history is retrieved through RANSAC estimation. From this data the instant drone velocity of 9.9 m/s is extracted with Doppler rate 225 Hz/s. Fig. 2*b* shows the range compressed result for the ground scene of four CRs, where the coherent processing interval (CPI) of target 1 is traced that corresponds to Fig. 2*a*. Similarly, the phase estimation and correction processes are performed for CR 2, 3 and 4 targets that lead to velocity estimation of 10.9, 12.3 and 13.1 m/s, respectively. As the platform is easily affected by the atmospheric turbulence and unstable flight scenario, the forward velocity and Doppler parameters are conceived as non-linear time-varying functions.

Fig. 1 *Drone SAR imaging field test*

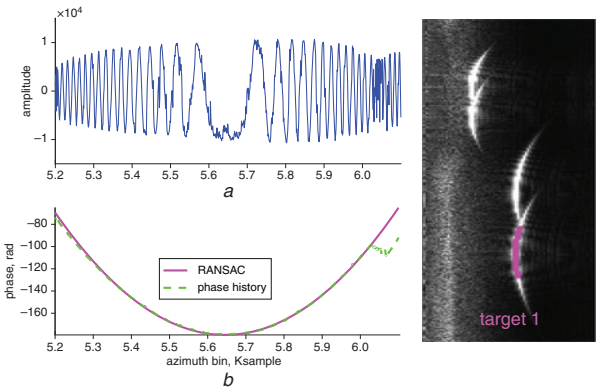

Fig. 2 *Range compressed drone SAR data of ground CR targets*
a Amplitude and phase history with RANSAC correction (target 1)
b Range compressed image

NUFFT for velocity interpolation: The coarse movement of multi-rotor platform leads to irregular sampling of the echo signals and makes it difficult to apply a direct fast Fourier transform (FFT) operation. In this Letter, a NUFFT algorithm is employed to activate fast SAR azimuth processing and rapid image acquisition. Previously, a periodic NUFFT has been considered for multi-channel SAR [3]. However, an alternative approach should be considered to reflect drone's non-periodic movements over extended trajectories.

As the velocity variation becomes severe, the sampling grids appear as non-uniform in both time and frequency domains and should be interpolated simultaneously. In this respect, the type 3 NUFFT is useful as it can freely choose the sampling grids in both domains [4].

To this purpose, the range compressed data $S(x)$ in Fig. 2 is converted into a discrete function $S[j]$. In this conversion, $S(x)$ is assumed to have been arbitrarily sampled at $x = x_j$ ($j = 0, 1, \ldots, N-1$), where x is a function of drone's forward velocity. A Gaussian function is chosen as the interpolation kernel, as its Fourier transform exhibit Gaussian property.

A transfer function $S_\tau(x)$ is defined by convolving $S(x)$ with the Gaussian $g_\tau(x) = \exp[-x^2/(4\tau)]$. Then the equispaced sample of $S_\tau(x)$ is

$$S_\tau(n\Delta_x) = \sum_{j=0}^{N-1} S[j] g_\tau(n\Delta_x - x_j) \tag{1}$$

Here, Δ_x is the sample grid in a uniform mesh and determined by the Gaussian constant τ. The type 3 NUFFT employs a transform function

$$S_\tau^{-\sigma}(x) = \frac{1}{\sqrt{2\sigma}} e^{\sigma x^2} \cdot S_\tau(x) = \frac{S_\tau(x)}{G_\sigma(x)} \tag{2}$$

$G_\sigma(x) = \sqrt{2\sigma} e^{-x^2\sigma}$ is equivalent to the Fourier transform of $g_\sigma(x)$ and used as amplitude pre-compensation. σ is an arbitrary positive constant. Then the Fourier transform of $S_\tau^{-\sigma}(x)$, designated as $\widetilde{S_\tau^{-\sigma}}(f)$, can be approximately calculated by the standard FFT on a uniform grid of Δ_f

as [4]

$$\widetilde{S_\tau^{-\sigma}}[m\Delta_f] \approx \frac{\Delta_x}{\sqrt{2\pi}} \sum_{n=0}^{N-1} S_\tau^{-\sigma}(n\Delta_x) \exp(-imn\Delta_x\Delta_f) \quad (3)$$

In (2), the Fourier transform of $S_\tau(x)$ is given as the convolution of given as $\widetilde{S_\tau}(f) = (\widetilde{S_\tau^{-\sigma}}(f) * g_\sigma(f))$ and can be calculated by replacing $\widetilde{S_\tau^{-\sigma}}(f)$ with (3). As $S_\tau(x)$ is the convolution of S and g_τ in spatial domain, the NUFFT of the original $S[j]$ can be expressed at $f = f_k$ by

$$\tilde{S}[f_k] \approx \frac{S_\tau(f_k)}{G_\tau(f_k)} = \frac{1}{\sqrt{2\tau}} e^{\tau(f_k)^2} \cdot \tilde{S}(f_k) \quad (4)$$

Hence, the discrete FFT of the non-uniformly sampled data set $S[j]$ is obtained using simple arithmetic operations. The accuracy of this approximation is affected by the interpolation length τ and the sampling grids of Δ_x, Δ_f. However, the sampling grid is no more constant when the velocity disturbance becomes severe and should be adjusted in accordance with the time-varying CPI. Then, the chirp rate k_a of the azimuth reference function is obtained by the interpolated velocity V_i as

$$k_a \approx \frac{2(V_i)^2}{\lambda R} = \frac{2}{\lambda} \cdot \left(\frac{\Delta_x \cdot N}{\mathrm{CPI}} \right)^2 \quad (5)$$

The spatial sampling grid Δ_x is dependent on the instant platform velocity. When its variation span is wide, the sampling parameters Δ_x, τ and Δ_f should be modified accordingly.

Experimental drone SAR data processing: The reference Doppler parameters are derived from the phase history in Fig. 1 and employed for azimuth processing to produce amplitude profiles for all targets as shown in Fig. 3. While the SAR focusing is effective for the target that corresponds to the reference function, other targets responses suffer from de-focusing and processing losses up to 2 dB in proportion to the velocity discrepancy.

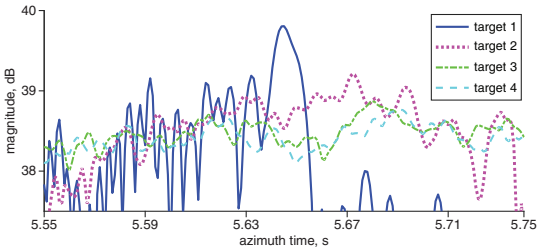

Fig. 3 *Azimuth profiles for ground targets*

For a fast and efficient compensation of this problem, the NUFFT processing is applied on the non-uniform azimuth signal. After the velocity distribution $v(t)$ is estimated, the range compressed data is converted into $S(x)$ in (1), where $x = v(t)\,\mathrm{d}t$.

To minimise velocity error accumulation, the azimuth data needs division into M multiple sub-apertures having separate NUFFT blocks. Here, M can be set as 4 by the number of CR targets. However, for a simple and fast processing, a single uniform grid is adopted by taking the sub-aperture interval of minimum velocity as reference. Afterward, the four sub-apertures are processed as one single NUFFT block. Here, the estimated velocity of 9.9 m/s from Fig. 1 is taken as the initial reference for grid interpolation. The Gaussian interpolation interval is determined by compromising the calculation accuracy and processing time. Here, they are selected as $\tau \approx 2.4\Delta_x$ and $\sigma \approx 2.4\Delta_f$. Then, the number of sampling grids in each sub-aperture ranges from 1900 to 2100. NUFFT calculation for the whole block takes <0.5 s, while pursuing an exact solution will be a time-consuming process.

For verification, Fig. 4 compares the final SAR images processed with and without velocity compensation. In Fig. 4*a*, inaccurate velocity estimation has resulted in blurring effects and geometric distortion errors. By comparison, Fig. 4*b* is obtained by employing NUFFT interpolation to carry out time-varying velocity compensation. The geometric errors of CR locations are corrected and the de-focussed blurring is suppressed.

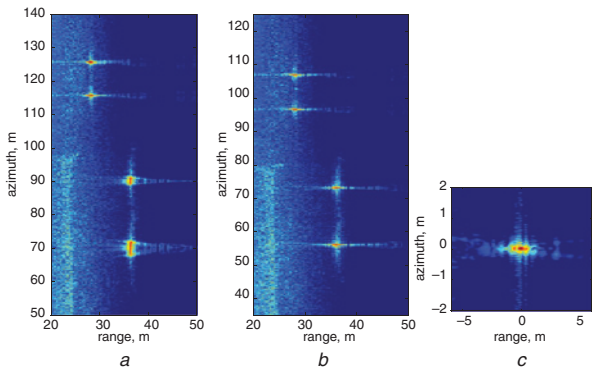

Fig. 4 *Drone SAR image*

a With velocity errors
b With non-uniform velocity compensation
c After residual phase error correction of target 1

It is equivalent to coarse motion compensation (MOCO) and can be performed with high efficiency through near-real-time processing at the azimuth resolution of 0.2 m. After residual phase error correction at post-processing, it is further enhanced to the theoretical limit of 0.1 m as shown in Fig. 4*c*.

Conclusion: The feasibility of micro-drone SAR is experimentally demonstrated using a portable FMCW radar system. Without navigation equipment, the complex movement of a lightweight drone platform has been efficiently compensated to generate high-resolution SAR images. The use of NUFFT enables to perform a coarse MOCO to compensate for the severe velocity variations and achieve near-real-time processing.

Acknowledgment: This work was supported by 2016 Korea Aerospace University faculty research grant.

Submitted: *3 March 2017* E-first: *20 April 2017*
doi: 10.1049/el.2017.0801
One or more of the Figures in this Letter are available in colour online.

W.K. Lee and K.W. Lee (*Department of Electronics & Information Engineering, Korea Aerospace University, Goyang-si, Gyenggi-do, South Korea*)

✉ E-mail: wklee@kau.ac.kr

References

1 Yan, X., Chen, J., Liyanage, P., *et al.*: 'A light-weight SAR system for multi-rotor UAV platform using LFM quasi-CW waveform'. IEEE IGARSS, Beijing, 2016, pp. 7346–7349, doi: 10.1109/IGARSS.2016.7730916
2 Zhou, S., Yang, L., Zhao, L., and Bi, G.: 'Forward velocity extraction from UAV raw SAR data based on adaptive notch filtering', *IEEE Trans. Geosci. Remote Sens. Lett.*, 2016, **13**, (9), pp. 1211–1215, doi: 10.1109/LGRS.2016.2576359
3 Lee, J.-Y., and Greengard, L.: 'The type 3 nonuniform FFT and its applications', *J. Comput. Phys.*, 2005, **206**, pp. 1–5
4 Zhao, S., Wang, R., Deng, Y., *et al.*: 'Modifications on multichannel reconstruction algorithm for SAR processing based on periodic nonuniform sampling theory and nonuniform fast Fourier transform', *J. Sel. Top. Appl. Earth Obs. Remote Sens.*, 2015, **8**, (11), pp. 4998–5006, doi: 10.1109/JSTARS.2015.2421303